Spectral functions of the Higgs mode near two-dimensional quantum critical points

Daniel Podolsky and Subir Sachdev

Spectral functions of the Higgs mode
near two-dimensional quantum critical points

Daniel Podolsky[1] and Subir Sachdev[2,3]

[1] *Physics Department, Technion, 32000 Haifa, Israel*
[2] *Department of Physics, Harvard University, Cambridge MA 02138, USA*
[3] *Instituut-Lorentz for Theoretical Physics, Universiteit Leiden,*
P.O. Box 9506, 2300 RA Leiden, The Netherlands
(Dated: July 30, 2012)

We study the Higgs excitation in the Goldstone phase of the relativistic $O(N)$ model in two spatial dimensions at zero temperature. The response functions of the order parameter, and its magnitude-squared, become universal functions of frequency in the vicinity of the quantum critical point described by the Wilson-Fisher fixed point, and we compute them to next-to-leading order in $1/N$. The Higgs particle has an infrared singular decay to gapless Goldstone excitations, and its response functions are characterized by a pole in the lower-half of the complex frequency plane. The pole acquires a non-zero real part only at next-to-leading order in $1/N$, demonstrating that the Higgs excitation has an oscillatory component even in the scaling limit. Both the real and imaginary parts of the pole position vanish with the correlation length exponent ν upon approaching the critical point. We present evidence that the spectral density of the $O(N)$-invariant amplitude-squared of the order parameter has a peak at a non-zero frequency in the scaling limit. We connect our results to recent experimental studies of the superfluid-insulator quantum phase transition of ultracold bosonic atoms in optical lattices.

I. INTRODUCTION

Quantum critical points described by relativistic field theories have long been the focus of theoretical study in condensed matter physics.[1–7] A number of experimental realizations of such critical points have also appeared in recent years. The critical point of the quantum Ising model in spatial dimension $d = 1$ has been realized in the ferromagnetic insulator[8] $CoNb_2O_6$, and also in tilted lattices[9] of ultracold bosons.[10] Neutron scattering experiments[11] on pressure-tuned $TlCuCl_3$ have mapped the excitations across the quantum critical point associated with the onset of Néel order in a dimerized antiferromagnet in $d = 3$. The organic insulator $(TMTTF)_2PF_6$ has a quantum phase transition[12] involving onset of Néel order under pressure in $d = 2$, but the excitations have not yet been completely studied. And ultracold bosonic atoms in optical lattices provide remarkable tunable realizations[13,14] of the superfluid-Mott insulator quantum phase transition in $d = 2$ and $d = 3$, whose properties can be studied closely using *in situ* imaging techniques.[15–19]

This paper will study the excitation spectrum in the vicinity of the quantum critical point of the relativistic $O(N)$ model in two spatial dimensions. The critical point itself is a conformal field theory in three spacetime dimensions (a CFT3), associated with the Wilson-Fisher fixed point.[20] Extensive studies of the excitation spectrum have appeared in previous work,[1,3–5,7] both at $T = 0$ and $T > 0$. Our focus here will be on the nature of the amplitude ('Higgs') excitation in the Goldstone phase with broken $O(N)$ symmetry at $T = 0$. It is generally believed that the excitation structure of this Goldstone phase is well understood, with $N - 1$ gapless Goldstone modes which behave like free particles at long wavelengths. However, there remain key open questions on the nature of the amplitude mode. In mean field theory, there is a sharp, gapped excitation in the longitudinal response, which may be identified with the Higgs particle. Beyond the mean field level, this excitation can emit multiple Goldstone excitations even at $T = 0$, and so the stability of the Higgs is not guaranteed. The Higgs has been argued[21,22] to be marginally stable in $d = 3$. In $d = 2$, there are infrared singularities[3–5] in the spin wave emission process, which indicate that the longitudinal response is overdamped, and imply that the ultimate nature of the amplitude mode is a strong-coupling problem. The

question of whether a finite frequency peak appears at the Higgs energy can depend[7,23] upon the specific observable being used to probe the amplitude mode.

Here, we will present a $1/N$ expansion of the spectrum of the Higgs excitation to next-to-leading order, and find some qualitatively new features. We show that the Higgs response functions are characterized by a pole in the lower-half complex frequency plane, and this pole acquires a non-zero real part at order $1/N$. We also find an associated structure in the spectral functions on the real frequency axis. Our results can serve as tests of the strong-coupling dynamics of the CFT3 in experiments. For instance, recent experiments on ultracold bosons in a optical lattices[19] have studied the low energy response near the $2d$ Mott-superfluid phase transition, described at integer boson filling by an $O(2)$ critical point with relativistic dynamics in 2+1 dimensions.

We represent the O(N) order parameter field by the N-component real field ϕ_α, with $\alpha = 1 \ldots N$. Let us orient the condensate in the Goldstone phase in the $\alpha = N$ direction, so that $\langle \phi_\alpha \rangle \propto \delta_{\alpha,N}$. As emphasized in a recent paper,[7] it is useful to consider two separate observable probes of the Higgs spectrum of fluctuations about this condensate.

The first observable concerns the longitudinal fluctuation of the order parameter, represented by ϕ_N, and we denote its connected two-point correlator by the susceptibility χ, where

$$\chi(p) = \int d^3x\, e^{-i\boldsymbol{p}\cdot\boldsymbol{x}} \left[\langle \phi_N(\boldsymbol{x})\phi_N(0) \rangle - \langle \phi_N(\boldsymbol{x}) \rangle \langle \phi_N(0) \rangle \right] \tag{1.1}$$

where $\boldsymbol{x}$ is a spacetime co-ordinate, $\boldsymbol{p}$ is spacetime momentum. We will work largely in imaginary time, and represent $p \equiv |\boldsymbol{p}|$, $x \equiv |\boldsymbol{x}|$, etc. The real time retarded response function, $\chi(\omega)$ is obtained by the analytic continuation $p \to -i\omega$ where ω is a measurement frequency and the momentum is zero. (Because of the relativistic invariance of the theory at $T = 0$, the susceptibility at non-zero momenta k can be deduced by $\omega \to \sqrt{\omega^2 - k^2}$.) The longitudinal susceptibility $\chi(\omega)$ is connected to the neutron scattering cross-section for experimental realizations in quantum antiferromagnets.

The second observable, the scalar susceptibility, is associated with two-point correlations of the O(N) invariant amplitude-squared of the order parameter $\sum_{\alpha=1}^{N} \phi_\alpha^2$ (in subsequent expression we will omit the summation sign, and use an implicit Einstein convention for summation over repeated indices). Specifically, we consider the response function

$$S(p) = \frac{1}{N} \int d^3x\, e^{-i\boldsymbol{p}\cdot\boldsymbol{x}} \left[\langle \phi_\alpha^2(\boldsymbol{x})\phi_\beta^2(0) \rangle - \langle \phi_\alpha^2(\boldsymbol{x}) \rangle \langle \phi_\beta^2(0) \rangle \right] \tag{1.2}$$

and its analytic continuation $S(\omega)$ after $p \to -i\omega$. Our main results concern the structure of the function $S(\omega)$ in the vicinity of the quantum critical point. The recent experiments on ultracold bosons in optical lattices[19] measure the imaginary part, $S''(\omega)$, by determining the energy absorption rate under periodic oscillations in the strength of the lattice potential, which induce an oscillation in the hopping matrix element of the bosons.

The susceptibility $\chi(\omega)$ was computed in Refs. 3–5. In the Goldstone phase, it was found that there was a zero frequency peak in the imaginary part $\chi''(\omega)$, with $\chi''(\omega) \sim 1/\omega$, and no finite ω peak which could indicate the energy of the Higgs excitation. When considered as an analytic function of a complex frequency ω, the retarded response function $\chi(\omega)$ was found to have a pole in the lower-half plane at a purely imaginary frequency, indicating that the Higgs mode was purely relaxational. We will compute the leading $1/N$ corrections to these results in our paper. We continue to find that $\chi''(\omega) \sim 1/\omega$ at small ω. However, a qualitatively new feature does emerge in the location of the pole in the lower-half complex plane: it now appears at a frequency which has a non-zero real part, indicating an oscillatory component to the Higgs excitation.

In the Goldstone phase, the response function $S(\omega)$ also has a pole in the lower-half frequency plane at precisely the same location as that for $\chi(\omega)$. However, now the oscillatory nature of the pole has a more visible signature on the real frequency axis. Previous work[3,7] found the imaginary part behaves as $S''(\omega) \sim \omega^3$ at small ω. At larger ω, no peak-like structure was found in the $N = \infty$ computation in the strict scaling limit; this scaling limit is taken by including only the single relevant perturbation away from the CFT3. Ref. 7 carried out computations beyond the scaling limit at $N = \infty$, and found a finite ω peak, representing the first signature of a Higgs-like excitation. In the present paper we will compute $S(\omega)$ to order $1/N$. We find evidence for a finite-ω peak in $S''(\omega)$ even in the strict scaling limit. The issue of whether the peak in $S''(\omega)$ appears in the scaling limit, or not, is important because it determines the manner in which the peak frequency, ω_p vanishes upon approaching the quantum critical point. A peak obtained in the scaling limit will have $\omega_p \sim (g_c - g)^\nu$, where ν the usual correlation length exponent, and g is the coupling constant tuning across the quantum critical point at $g = g_c$ (here the dynamic critical exponent $z = 1$). Different behavior is expected for a peak which appears only because of corrections to scaling: in this case we can estimate from the results in Ref. 7 that $\omega_p \sim (g_c - g)^{\nu(1-\varpi)}$, where ϖ is the leading correction to scaling exponent at the Wilson-Fisher fixed point.[24] Another key difference between the two types of peak is found in the behavior of the width of the peak, γ, as one approaches the critical point. For a peak obtained in the scaling limit, the ratio γ/ω_p is fixed, and hence γ must necessarily go to zero at the critical point. In contrast, for a peak which appears only due to

corrections to scaling, γ will in general not vanish at the critical point.

While our paper was being completed, we learnt of the numerical study of Pollet and Prokof'ev[25]. They found a peak in $S''(\omega)$ which appeared to vanish as $\omega_p \sim (g_c - g)^\nu$; this is further evidence that a peak is present already in the scaling limit.

We will present our scaling limit results for $S(\omega)$ (and $\chi(\omega)$) in terms of universal scaling functions. As in the analysis of Ref. 26 for the quantum phase transition in the $d = 3$ coupled-dimer antiferromagnet, it is useful to normalize the universal structure in the energy scale by comparing the response functions on systems located symmetrically on opposite sides of the critical point. Thus let us take a point in the gapped phase with $O(N)$ symmetry preserved with $g = g_+ > g_c$. Then its partner point with $g = g_- < g_c$ is determined by

$$g_+ - g_c = g_c - g_- \tag{1.3}$$

Let Δ be the *exact* energy gap to single-particle excitations in the symmetric phase at $g = g_+$; consequently there is a pole in $\chi(\omega)$ at the real frequency $\omega = \Delta$ for $g = g_+$:

$$\frac{\omega_{\text{pole}}}{\Delta} = 1 \quad , \quad g = g_+, \tag{1.4}$$

and this defines the value of Δ. By the definition of the critical exponent ν, $\Delta \sim (g_+ - g_c)^\nu$ upon approaching g_c. Note that our definition of Δ is such that the threshold of $S''(\omega)$ in the symmetric phase occurs at 2Δ; for applications to the superfluid-insulator transition, Δ is the gap in the single boson Green's function in the Mott phase. We will use Δ to set the energy scale of *all* excitations, including those at $g = g_-$.

For $g = g_-$, a key signature of the retarded response functions $\chi(\omega)$ and $S(\omega)$ is their common lower-half complex plane pole. Its location, ω_{pole}, is completely determined by Δ, and we find

$$\frac{\omega_{\text{pole}}}{\Delta} = -i\frac{4}{\pi} + \frac{1}{N}\left(\frac{16\left(4 + \sqrt{2}\log\left(3 - 2\sqrt{2}\right)\right)}{\pi^2} + 2.46531203396\,i\right) + \mathcal{O}(1/N^2) \quad , \quad g = g_-. \tag{1.5}$$

The purely imaginary $N = \infty$ result was obtained earlier[3]. Note the key appearance of a real part $\sim 2.443216943237169/N$ in the $1/N$ correction, which is a measure of the oscillatory component of the Higgs excitation.

We have claimed above that $\chi(\omega)$ and $S(\omega)$ have the same pole structure in the lower-half complex frequency plane for $g = g_-$. This is a consequence of the broken $O(N)$ symmetry, which mixes together the fluctuations of the longitudinal component and the amplitude-squared of the order parameter. This will be evident from the structure of our analysis in Section IV. In contrast, in the symmetric gapped phase $g = g_+$, these two observables have very different analytic structures. While $\chi(\omega)$ has a pole on the real frequency axis, as in Eq. (1.4), the singularity of $S(\omega)$ is quite distinct. This response function is in the two-particle sector, and so for $g = g_+$ it has a threshold singularity at $\omega = 2\Delta$, as we noted above. We will show that this threshold singularity is of the form

$$S''(\omega) = \frac{\widetilde{\mathcal{A}}\,\Delta^{3-2/\nu}}{\ln^2\left(\frac{4\Delta}{(|\omega| - 2\Delta)}\right)}\,\text{sgn}(\omega)\,\theta(|\omega| - 2\Delta) \quad , \quad g = g_+. \tag{1.6}$$

Here $\widetilde{\mathcal{A}}$ is a non-universal cut-off dependent prefactor which depends upon the precise definition of ϕ_α, and which can be replaced by a constant in the vicinity of the critical point.

We also compute the universal structure of the amplitude-squared response function, $S(\omega)$, on the real frequency axis in the Goldstone phase with $g = g_-$. Here there is no threshold, and we have $S''(\omega) \sim \omega^3$ as noted above. More precisely we find

$$S''(\omega) = \mathcal{A}\,\Delta^{-2/\nu}\omega^3 \quad \text{for} \quad \omega \to 0, \; g = g_-. \tag{1.7}$$

where $\mathcal{A}$ is another non-universal cut-off dependent constant prefactor, and Δ is defined as always by Eq. (1.4). The recent observation of the low frequency spectrum in ultracold atom experiments[19] are consistent with the scaling in Eq. (1.7). The ratio of the amplitudes of the low frequency singularities at $g_\pm$ in Eqs. (1.6) and (1.7) are universal, and we find to order $1/N$ (from Eqs. (3.10) and (4.16)) that

$$\frac{\widetilde{\mathcal{A}}}{\mathcal{A}} = 32\left(1 + \frac{4.099}{N}\right) + \mathcal{O}(1/N^2). \tag{1.8}$$

3

For general ω, the scaling limit structure of $S(\omega)$ is (see the end of Sec. II)

$$S(\omega) \sim \text{constant} + \Delta^{3-2/\nu} \Phi(\omega/\Delta), \tag{1.9}$$

where Φ is a universal function which we will compute here to order $1/N$; the missing proportionality constant in Eq. (1.9) can be fixed by demanding consistency with Eqs. (1.6,1.7) for $g = g_\pm$, and the additive constant is a non-universal real number. We will find evidence that in the Goldstone phase ($g = g_-$) the function Φ has a peak as a function of ω, which can be taken as an additional signature of the Higgs mode in two spatial dimensions. For small ω, the corrections to Eq. (1.7) are in Eq. (4.15) and these are schematically

$$S''(\omega) \sim \omega^3 + \omega^5 \log(\omega). \tag{1.10}$$

This non-analytic correction is significant, and a signature of the strong coupling to the gapless modes. Associated non-analytic terms are responsible for the real part of the pole of $S(\omega)$ in Eq. (1.5), as will become evident from the discussion in Section V.

We will begin by setting up the general formalism for the $1/N$ expansion for the Wilson-Fisher fixed point in Section II. We will show here that the correlators of ϕ_α^2 can be efficiently computed by relating them to the correlators of an auxillary scalar field. We will then apply this method to computations in the gapped phase, $g = g_+$, in Section III. Our main results for the amplitude excitations of the Goldstone phase, $g = g_-$, appear in Section IV. We present a unified review of our results in Section V.

II. GENERAL FORMALISM

In this section, we set up some general formalism for the $O(N)$ model. We will be interested in the field theory

$$Z_u[J] = \int \mathcal{D}\phi_\alpha \exp\left(-\int_{\boldsymbol{x}} \left[\frac{1}{2}(\partial\phi_\alpha)^2 + \frac{u}{2N}\left(\phi_\alpha^2 - N/g\right)^2 + J\phi_\alpha^2\right]\right) \tag{2.1}$$

where $\int_{\boldsymbol{x}} \equiv \int d^3x$, u is a quartic non-linearity, and g is the tuning parameter across the transition. We have included a spacetime dependent source for the amplitude-squared mode, $J(\boldsymbol{x})$, and will eventually set $J(\boldsymbol{x}) = 0$ after taking functional derivatives of $Z_u(J)$. Note that the partition function in Eq. (2.1) is just the standard ϕ^4 field theory of the Wilson-Fisher fixed point, in an unconventional notation; the notation is designed to simplify the large N limit, and to make a natural connection to the fixed length non-linear sigma model in the limit $u \to \infty$.

We decouple the quartic term, and write the partition function as

$$Z_u[J] = \int \mathcal{D}\phi_\alpha \mathcal{D}\widetilde{\lambda} \exp\left(-\frac{1}{2}\int_{\boldsymbol{x}} \left[(\partial\phi_\alpha)^2 + \frac{i}{\sqrt{N}}\widetilde{\lambda}\left(\phi_\alpha^2 - N/g\right) + \frac{\widetilde{\lambda}^2}{4u} + 2J\phi_\alpha^2\right]\right) \tag{2.2}$$

In the large N limit, we perform the Gaussian functional integral over ϕ_α (at $J = 0$), and expand the fluctuations in $\widetilde{\lambda}$ about the saddle point of the effective action. In the symmetric phase, the saddle point is at $i\widetilde{\lambda}/\sqrt{N} = r$, where

$$\frac{1}{g} + \frac{r}{2u} = \int_{\boldsymbol{p}} \frac{1}{p^2 + r}, \tag{2.3}$$

where $\int_{\boldsymbol{p}} \equiv \int d^3p/(8\pi^3)$. The nature of the saddle point in the Goldstone phase will be discussed later. So we write $\widetilde{\lambda} = -i\sqrt{N}r + i2\sqrt{N}J + \lambda$, and completely integrate out the ϕ_α field. Then, the effective action for λ is

$$Z_u[J] = \int \mathcal{D}\lambda \exp\left(-\mathcal{S}_J - \mathcal{S}_0 - \mathcal{S}_1\right)$$

$$\mathcal{S}_0 = \frac{1}{2}\int_{\boldsymbol{p}} \left(\frac{\Pi(p,r)}{2} + \frac{1}{4u}\right)\lambda^2$$

$$\mathcal{S}_J = -\frac{Nr}{2g} - \frac{Nr^2}{8u} + \int_{\boldsymbol{x}} \left[J \frac{\left(Nr + 2Nu/g + i\sqrt{N}\lambda\right)}{2u} - \frac{NJ^2}{2u}\right] \tag{2.4}$$

where $\mathcal{S}_1$ involves cubic and higher order terms in λ alone, and is specified in Appendix A; we note that $\mathcal{S}_1$ is

4

independent of u. We show in Appendix B that r plays the role of the tuning parameter away from the quantum critical point, with $r \sim (g - g_c)^2$ for $g > g_c$.

Now we can take functional derivatives w.r.t. J, and obtain the two-point correlator of ϕ_α^2 at $J = 0$ as

$$\langle \phi_\alpha^2(\boldsymbol{x})\phi_\beta^2(0)\rangle - \langle \phi_\alpha^2\rangle^2 = \frac{N}{u}\delta^d(\boldsymbol{x}) - \frac{N}{4u^2}\left[\langle \lambda(\boldsymbol{x})\lambda(0)\rangle - \langle \lambda\rangle^2\right] \tag{2.5}$$

So we see that the amplitude-squared correlator, $S(p)$, is simply proportional to the two-point correlator of the λ field. Specifically, we will identify

$$S(\omega) \equiv \text{constant} - G_{\lambda\lambda}(\omega) \tag{2.6}$$

where the right hand side contains the connected λ Green's function, and we are not interested in the additive non-universal constant. The function $G_{\lambda\lambda}(\omega)$ will be computed in this paper in the $1/N$ expansion; this expansion can be carried out at any value of u, including the theory in which we impose the fixed length limit by taking the $u \to \infty$ limit. We also note that the identity (2.5) also holds in the Goldstone phase. Having proved (2.5), we will set $J = 0$ is all subsequent computations.

In the symmetric phase, $g > g_c$, we can write the λ Green's function as

$$[G_{\lambda\lambda}(p)]^{-1} = [G_{\lambda\lambda}^0(p)]^{-1} - \Sigma_{\lambda\lambda}(p) \tag{2.7}$$

The bare propagator is

$$G_{\lambda\lambda}^0(p) = \frac{2}{\Pi(p, r) + 1/(2u)} \tag{2.8}$$

where

$$\Pi(p, r) = \int_{\boldsymbol{q}} \frac{1}{(q^2 + r)((\boldsymbol{p} + \boldsymbol{q})^2 + r)} = \frac{1}{4\pi p}\tan^{-1}\left(\frac{p}{2\sqrt{r}}\right)$$

$$= \frac{1}{8\pi p i}\ln\left(\frac{2\sqrt{r} + ip}{2\sqrt{r} - ip}\right) \tag{2.9}$$

Note that $\Pi(p, r)$ diverges as $p, r \to 0$, and so the $1/(2u)$ term in Eq. (2.8) can be neglected in this limit. Because u does not appear in the non-linear terms in $\mathcal{S}_1$, we need to send $u \to \infty$ to obtain the scaling limit, and we will do so in most of our expressions; thus the scaling limit response function in the vicinity of the quantum critical point is the same for the "soft spin" (finite u) and fixed length ($u = \infty$) theories. In terms of the expressions obtained in Appendix A, the expression for the self energy to order $1/N$ is

$$\Sigma_{\lambda\lambda}(p) = -\frac{1}{2N}\int_{\boldsymbol{k}}\left[K_3(p, k, |\boldsymbol{p} + \boldsymbol{k}|)\right]^2 G_{\lambda\lambda}^0(|\boldsymbol{k} + \boldsymbol{p}|)G_{\lambda\lambda}^0(k)$$

$$- \frac{1}{2N}K_3(p, -p, 0)G_{\lambda\lambda}^0(0)\int_{\boldsymbol{k}}K_3(\boldsymbol{k}, -\boldsymbol{k}, 0)G_{\lambda\lambda}^0(k)$$

$$+ \frac{1}{6N}\int_{\boldsymbol{k}}K_4(\boldsymbol{p}, \boldsymbol{k}, -\boldsymbol{p}, -\boldsymbol{k})G_{\lambda\lambda}^0(k) + \frac{1}{3N}\int_{\boldsymbol{k}}K_4(\boldsymbol{p}, -\boldsymbol{p}, \boldsymbol{k}, -\boldsymbol{k})G_{\lambda\lambda}^0(k). \tag{2.10}$$

We can also obtain the expression for the ϕ_α Green's function, $G(p)$, by similar methods. To order $1/N$ we obtain

$$G^{-1}(p) = p^2 + r + \frac{1}{N}\int_{\boldsymbol{q}}G_{\lambda\lambda}^0(q)\frac{1}{((\boldsymbol{p} + \boldsymbol{q})^2 + r)}$$

$$- \frac{1}{2N}G_{\lambda\lambda}^0(0)\int_{\boldsymbol{k},\boldsymbol{q}}\frac{1}{(k^2 + r)^2((\boldsymbol{k} + \boldsymbol{q})^2 + r)}G_{\lambda\lambda}^0(q). \tag{2.11}$$

We describe the structure of the critical singularities, as g approaches g_c, in the expressions in Eqs. (2.10) and (2.11) in Appendix B.

Before proceeding further, we give a brief derivation of Eq. (1.9), which plays a central role in our analysis. Consider the $D = 3$ dimensional statistical mechanics model defined by the partition function in Eq. (2.1), and define the free

energy density $f \equiv -\frac{1}{V} \ln Z_u[J = 0]$. Then, taking two derivatives of f with respect to g^{-1} we obtain,

$$\frac{\partial^2 f}{(\partial g^{-1})^2} = -uN + \frac{u^2}{V} \int_{\boldsymbol{x},\boldsymbol{y}} \left[\langle \phi_\alpha^2(\boldsymbol{x}) \phi_\beta^2(\boldsymbol{y}) \rangle - \langle \phi_\alpha^2(\boldsymbol{x}) \rangle \langle \phi_\beta^2(\boldsymbol{y}) \rangle \right] \tag{2.12}$$

which is the $p = 0$ Matsubara frequency correlation function $S(p = 0)$, up to additive and multiplicative constants. On the other hand, near the critical point g_c, f can be split into regular and singular parts, $f = f_{reg} + f_{sing}$ where, according to the hyperscaling hypothesis, $f_{sing} \sim \xi^{-D}$. Here, the correlation length $\xi \sim |g - g_c|^{-\nu}$ or, equivalently, $\xi \sim |g_c^{-1} - g^{-1}|^{-\nu}$. By taking two derivatives of f_{sing} with respect to g^{-1}, we conclude

$$S(p = 0) \sim \xi^{-D+2/\nu} + (\text{regular constant}) \tag{2.13}$$

Finally, since $\xi \propto 1/\Delta$ for a relativistic theory, and generalizing this result to arbitrary real frequencies, we obtain

$$S(\omega) \sim \Delta^{3-2/\nu} \Phi(\omega/\Delta) + \text{constant}, \tag{2.14}$$

which is Eq. (1.9).

III.   SPECTRAL FUNCTIONS IN THE SYMMETRIC PHASE

This section limits attention to the gapped phase where the O(N) symmetry is preserved, present for $g > g_c$. The dominant singularity in the ϕ_α propagator is the pole corresponding to the N-fold degenerate particle excitation. Let us determine the position and residue of this pole to order $1/N$.

The quasiparticle pole is determined by the solution of $G^{-1}(p) = 0$ where from (B9)

$$G^{-1}(p) = p^2 + r + \frac{1}{N\pi p} \int_0^\Lambda dq \frac{q^2}{\tan^{-1}(q/(2\sqrt{r}))} \left[\ln \left(\frac{(p+q)^2 + r}{(p-q)^2 + r} \right) - \frac{4pq}{q^2 + 4r} \right] \tag{3.1}$$

So the pole is at $p^2 = -\Delta^2$ where

$$\Delta^2 = r + \frac{1}{N\pi} \int_0^\Lambda dq \frac{q^2}{\tan^{-1}(q/(2\sqrt{r}))} \left[\frac{2}{\sqrt{r}} \tan^{-1} \left(\frac{2\sqrt{r}}{q} \right) - \frac{4q}{q^2 + 4r} \right] \tag{3.2}$$

The integral yields

$$\Delta^2 = r \left[1 + \frac{32}{3\pi^2 N} \left(\ln \left(\frac{\Lambda^2}{r} \right) + 0.50260886161586 \right) \right]. \tag{3.3}$$

This is the needed connection between the renormalized energy gap, Δ, and the bare tuning parameter r. Recall that we showed in Appendix B that $r \sim (g - g_c)^2$, and so $\Delta \sim (g - g_c)^\nu$ where

$$\nu = 1 - \frac{32}{3\pi^2 N}. \tag{3.4}$$

Also, we have[3] for the wavefunction renormalization $\mathcal{Z}$

$$
\begin{aligned}
\frac{1}{\mathcal{Z}} &= \left. \frac{dG^{-1}(p)}{dp^2} \right|_{p^2 = -\Delta^2} \\
&= 1 + \frac{1}{N\pi r} \int_0^\Lambda dq \frac{q^2}{\tan^{-1}(q/(2\sqrt{r}))} \left[\frac{1}{\sqrt{r}} \tan^{-1} \left(\frac{2\sqrt{r}}{q} \right) - \frac{q}{q^2 + 4r} - \frac{1}{q} \right] \\
&= 1 + \eta \left(\ln \left(\frac{\Lambda}{\sqrt{r}} \right) - 1.78297175565687 \right)
\end{aligned} \tag{3.5}
$$

where the critical exponent η is given by Eq. (B6).

A. Threshold singularity

As we discussed in Section I, the low frequency singularity in $G_{\lambda\lambda}$ is a threshold at a frequency 2Δ. So we consider the non-analytic terms in $G_{\lambda\lambda}(p)$ at $p = -i(2\Delta + \omega)$ as $\omega \to 0$.

At $N = \infty$ we have

$$
\begin{aligned}
G^0_{\lambda\lambda}(p) &= \frac{2}{\Pi(-2i\sqrt{r} - i\omega, r)} \\
&= \frac{32\pi\sqrt{r}}{\ln\left(\frac{4\sqrt{r}}{-\omega}\right)}
\end{aligned}
\tag{3.6}
$$

So near threshold we have

$$
\mathrm{Im}G^0_{\lambda\lambda}(p) = \frac{32\pi^2\sqrt{r}}{\ln^2(4\sqrt{r}/|\omega|)}\theta(\omega)
\tag{3.7}
$$

The $1/\ln^2$ prefactor is easy to understand. We are considering the creation of two slowly moving particles in two dimensions with a k^2 dispersion at low momenta; such particles have a well-known logarithmic singularity in their T-matrix for short-range interactions.[22] This argument also implies that the $1/\ln^2$ prefactor will be robust at higher orders at $1/N$, as we indeed find below.

At order $1/N$, we compute the threshold singularity in $G_{\lambda\lambda}$ from (2.10). Notice that the second and fourth terms in (2.10) can be absorbed into a self-energy renormalization of the ϕ_α propagator, which only contributes via the quasiparticle wavefunction renormalization to the threshold singularity. So for the purposes of the threshold singularity we can write

$$
G_{\lambda\lambda}(p) = \frac{2}{\mathcal{Z}^2\Pi(p, \Delta^2)} - \frac{8}{N\Pi^2(p, r)}\int_{\boldsymbol{k}}\frac{[K_3(p, k, |\boldsymbol{p}+\boldsymbol{k}|)]^2}{\Pi(|\boldsymbol{k}+\boldsymbol{p}|, r)\Pi(k, r)} + \frac{4}{3N\Pi^2(p, r)}\int_{\boldsymbol{k}}\frac{K_4(\boldsymbol{p}, \boldsymbol{k}, -\boldsymbol{p}, -\boldsymbol{k})}{\Pi(k, r)}
\tag{3.8}
$$

It remains to evaluate the $\boldsymbol{k}$ integrals in the limit $\omega \to 0$. We present details of this evaluation in Appendix C. The final result can be written as

$$
\mathrm{Im}G_{\lambda\lambda}(p) = \frac{\widetilde{\mathcal{A}}\Delta^{3-2/\nu}}{\ln^2(4\Delta/|\omega|)}\theta(\omega)
\tag{3.9}
$$

with the amplitude $\widetilde{\mathcal{A}}$ is that appearing in Eq. (1.6), and is given by

$$
\widetilde{\mathcal{A}} = 32\pi^2\Lambda^{2/\nu-2}\left(1 + \frac{1.481}{N} + \dots\right).
\tag{3.10}
$$

IV. SPECTRAL FUNCTIONS IN THE GOLDSTONE PHASE

We write $\phi_\alpha = (\sqrt{N}\sigma_0 + \sigma, \pi_i)$ with $i = 1\dots N-1$ where

$$
\sigma_0^2 = \frac{1}{g} - \int_{\boldsymbol{p}}\frac{1}{p^2},
\tag{4.1}
$$

is the condensate at $N = \infty$. From (1.3) and (B7), we can relate this to the value of r at the partner point in the symmetric phase

$$
\sigma_0^2 = \frac{\sqrt{r}}{4\pi}
\tag{4.2}
$$

where r is related to the single particle gap in the paramagnet via Eq. (3.3). This yields a relation between σ_0^2 and the gap at the partner point in the symmetric phase:

$$\sigma_0^2 = \frac{\Delta}{4\pi} - \frac{32\sigma_0^2}{3\pi^2 N} \ln\left(\frac{\Lambda}{16\sigma_0^2}\right) - \frac{\mathcal{C}\sigma_0^2}{N} \tag{4.3}$$

where $\mathcal{C} = 0.5326726500732776$. This can also be written as

$$\sigma_0^2 = \frac{\Delta}{4\pi}\left[1 - \frac{\mathcal{C}}{N} - \frac{32}{3\pi^2 N} \ln\left(\frac{\pi\Lambda}{4\Delta}\right)\right] \tag{4.4}$$

within the same order in $1/N$.

We can set $\widetilde{\lambda} = \lambda$ in Eq. (2.2), and then integrating over the π_i we obtain the partition function

$$
\begin{aligned}
Z &= \int \mathcal{D}\sigma \mathcal{D}\lambda \exp\left(-\mathcal{S}_0 - \mathcal{S}_1 - \mathcal{S}_2\right) \\
\mathcal{S}_0 &= \frac{1}{2} \int_{\boldsymbol{p}} \left[p^2\sigma^2 + 2i\sigma_0\sigma\lambda + \frac{1}{2}\Pi(p,0)\lambda^2\right] \\
\mathcal{S}_2 &= -\frac{i}{2\sqrt{N}}\left(\frac{1}{g} - \sigma_0^2\right)\int_x \lambda - \frac{1}{4N}\int_{\boldsymbol{p}} \Pi(p,0)\lambda^2 + \frac{i}{2\sqrt{N}}\int_x \lambda\sigma^2
\end{aligned} \tag{4.5}
$$

where $\mathcal{S}_1$ is just as in Appendix A but with $K_{3,4}$ evaluated at $r = 0$. Now the connected σ-σ Green's function is equivalent to the longitudinal susceptibility $\chi(\omega)$ introduced in Section I:

$$\chi(\omega) \equiv G_{\sigma\sigma}(\omega). \tag{4.6}$$

The bare connected Green's functions of (4.5) are

$$
\begin{aligned}
G_{\sigma\sigma}^0(p) &= \frac{\Pi(p,0)}{p^2\Pi(p,0) + 2\sigma_0^2} \\
G_{\lambda\lambda}^0(p) &= \frac{2p^2}{p^2\Pi(p,0) + 2\sigma_0^2} \\
G_{\sigma\lambda}^0(p) &= \frac{-2i\sigma_0}{p^2\Pi(p,0) + 2\sigma_0^2}
\end{aligned} \tag{4.7}
$$

The corresponding renormalized connected Green's functions require computations of the self-energies at order $1/N$, and these are presented in Appendix D.

Using the value of $\Pi(p,0)$ in Eq. (2.9), we see that all the Green's functions have poles at $p = -16\sigma_0^2$, which corresponds to the lower-half plane value $\omega = -i16\sigma_0^2$. After including the self-energies, this pole corresponds to the point where the effective quadratic action for λ and σ has a zero eigenvalue. Equivalently this is the condition that the determinant of the quadratic form vanish *i.e.*

$$\det\begin{pmatrix} p^2 - \Sigma_{\sigma\sigma}(p) & i\sigma_0 - \Sigma_{\sigma\lambda}(p) \\ i\sigma_0 - \Sigma_{\sigma\lambda}(p) & 1/(16p) - \Sigma_{\lambda\lambda}(p) \end{pmatrix} = 0 \tag{4.8}$$

where Σ are self energies computed in Appendix D. Note that upon ignoring the self-energies, the solution of Eq. (4.8) is indeed $p = -16\sigma_0^2$. Rather than solving this equation with self energies to next order in $1/N$, it is more convenient to locate the pole by examining the zero of $1/G_{\sigma\sigma}$, which we will do in Section IV B.

A. Computation of Φ

We can now use the results for the self energies computed in Appendix D to obtain expressions for the connected λ Green's functions to order $1/N$:

$$
\begin{aligned}
G_{\lambda\lambda}(p) &= G_{\lambda\lambda}^0(p) + \Sigma_{\lambda\lambda}(p)\left[G_{\lambda\lambda}^0(p)\right]^2 + \Sigma_{\sigma\sigma}(p)\left[G_{\lambda\sigma}^0(p)\right]^2 + 2\Sigma_{\lambda\sigma}(p)G_{\lambda\lambda}^0(p)G_{\lambda\sigma}^0(p) \\
&= \frac{16p^2}{p+16\sigma_0^2} + \frac{16p^3}{N(p+16\sigma_0^2)^2} + \frac{1024p^2(p+8\sigma_0^2)}{3\pi^2 N(p+16\sigma_0^2)^2}\ln\left(\frac{\Lambda}{16\sigma_0^2}\right) \\
&\quad + \frac{256\sigma_0^2}{(p+16\sigma_0^2)^2 N}\left[p^2 F_{\lambda\lambda}(p) - \sigma_0^4 F_{\sigma\sigma}(p) + 2p\sigma_0^2 F_{\sigma\lambda}(p)\right] \\
&\quad - \frac{256\Lambda}{\pi^2 N} + \frac{8192\sigma_0^2}{\pi^2 N}\ln\left(\frac{\Lambda}{16\sigma_0^2}\right),
\end{aligned} \tag{4.9}
$$

where the F functions are defined in Eqs. (D2-D4). The terms in the last line are p-independent real constants, and will be dropped since they do not contribute to $S''(\omega)$ upon using Eq. (2.6). After this subtraction, it is notable that all the terms linear in Λ have cancelled out of this expression, indicating that the $S(\omega)$ is universal near the quantum critical point.

In order to extract the universal scaling function Φ from $G_{\lambda\lambda}$, as introduced in Eq. (1.9), we first collect the p-independent terms appearing in the last line of Eq. (4.9). These terms are explicitly real and can be absorbed into the constant in Eq. (1.9). We then use Eq. (4.4) to substitute σ_0 by Δ, and find:

$$
\begin{aligned}
G_{\lambda\lambda}(p) &= (\text{const}) + \frac{16p^2}{p+4\Delta/\pi} + \frac{16p^2(p+4\mathcal{C}\Delta/\pi)}{N(p+4\Delta/\pi)^2} + \frac{1024p^2}{3\pi^2 N(p+4\Delta/\pi)}\ln\left(\frac{\pi\Lambda}{4\Delta}\right) \\
&\quad + \frac{4\Delta}{N\pi^3(p+4\Delta/\pi)^2}\left[16\pi^2 p^2 F_{\lambda\lambda}(p) - \Delta^2 F_{\sigma\sigma}(p) + 8\pi p\Delta F_{\sigma\lambda}(p)\right]
\end{aligned} \tag{4.10}
$$

Using

$$
(\Delta/\Lambda)^{2-2/\nu} = 1 + \frac{64}{3\pi^2 N}\ln(\Delta/\Lambda), \tag{4.11}
$$

this can be written as

$$
G_{\lambda\lambda}(p) = (\text{const}) + \Delta\,(\Delta/\Lambda)^{2-2/\nu}\,H_\lambda(p/\Delta) \tag{4.12}
$$

where

$$
\begin{aligned}
H_\lambda(p/\Delta) &= \frac{16p^2}{\Delta(p+4\Delta/\pi)} + \frac{16p^2(p+4\mathcal{C}\Delta/\pi)}{N\Delta(p+4\Delta/\pi)^2} + \frac{1024p^2}{3\pi^2 N(p+4\Delta/\pi)}\ln\left(\frac{\pi}{4}\right) \\
&\quad + \frac{4}{N\pi^3(p+4\Delta/\pi)^2}\left[16\pi^2 p^2 F_{\lambda\lambda}(p) - \Delta^2 F_{\sigma\sigma}(p) + 8\pi p\Delta F_{\sigma\lambda}(p)\right].
\end{aligned} \tag{4.13}
$$

Importantly, notice that all the logarithmic dependence upon the cutoff Λ has dropped out, yielding a universal expression for H_λ; this is a significant check on our computation. By comparing Eq. (4.12) to Eqs. (1.9) and (2.6), we see that the scaling function Φ is

$$
\Phi\left(\frac{\omega}{\Delta}\right) = -H_\lambda\left(\frac{-i\omega}{\Delta}\right). \tag{4.14}
$$

Hence, Φ is obtained from the analytic continuation of H_λ to $p = -i\omega$.

At small values of $z = \omega/\Delta$, the expansion (D5) yields

$$
\begin{aligned}
\Phi(z) &= \left(4\pi - \frac{25.898}{N}\right)z^2 + i\left(\pi^2 - \frac{25.842}{N}\right)z^3 + \left(-\frac{\pi^3}{4} + \frac{40.690}{N}\right)z^4 \\
&\quad + \left(-\frac{i\pi^4}{16} + \frac{50.584i}{N} - \frac{2i\pi^2}{3N}\ln(-iz)\right)z^5 + \mathcal{O}\left(z^6\right).
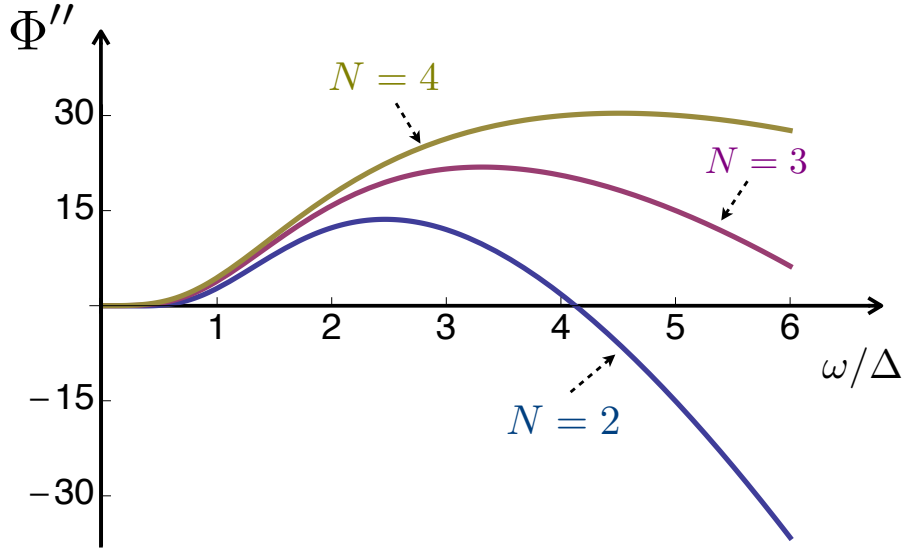\end{aligned} \tag{4.15}
$$

9

FIG. 1: Universal component of the scalar spectral function, $\Phi''(\omega/\Delta)$, for different values of N. The change of sign in the $N = 2$ curve at large ω/Δ is an artifact of the approximation being used.

Note that the imaginary part of Φ has a leading ω^3 behavior. This relies on a precise cancellation of a term $\sim \omega$, and is consistent with previous results[3,7]. The coefficient of ω^3 is a measure of the decay rate of the Higgs excitation into two gapless Goldstone modes. Comparing the definition in Eq. (1.7) with Eq. (4.15) we have

$$\mathcal{A} = \Lambda^{2/\nu-2}\left(\pi^2 - \frac{25.842}{N}\right). \tag{4.16}$$

Note that there is a branch cut in Eq. (4.15) at $\omega = 0$, as indicated to lowest order in ω by the term $\omega^5 \log \omega$. This is a non-analytic consequence of the presence of gapless excitations. This same non-analytic term is responsible for the real part of the pole in Eq. (1.5), as is shown in Appendix D and discussed in Section V.

We next evaluate Φ numerically at general values of ω. For this, we must perform an analytic continuation of the integrals F in Eqs. (D2-D4) to real frequency $p = -i\omega$. A Wick rotation of these integrals can be performed by taking $p = e^{-i\alpha}\omega$ and $k = e^{-i\alpha}\nu$, and varying α continuously from $\alpha = 0$ (the Euclidean time result) to $\alpha = \pi/2$ (real-time). On general grounds, we expect not to cross any singularities upon this Wick rotation – indeed, this can be verified explicitly by inspection of the integrands. Thus, we interpret $F(p = -i\omega)$ in Eqs. (D2-D4) as integrals along straight line segments on the complex plane, running from $k = 0$ to $k = -i\omega$, and from $k = -i\omega$ to $k = -i\infty$.

The universal scaling contribution to the scalar spectral function, $\Phi''(\omega/\Delta)$, is shown in Fig. 1 for $N = 2$, $N = 3$, and $N = 4$. Note that Φ'' has a peak in all cases. This is one of the main results of our analysis. It supports the appearance of the Higgs mode as a finite width peak in scalar measurements in the quantum critical region. The presence of this peak is substantiated by recent experiments[19] and quantum Monte-Carlo simulations[25] of the Mott-superfluid transition at integer filling of bosons, corresponding to the case $N = 2$.

The $N = 2$ curve in Fig. 1 is negative at large ω, and also at very low values of ω, as can be inferred from the sign of $\mathcal{A}$ in Eq. (4.16) for $N = 2$ (resulting in a very shallow negative region that cannot be discerned in the scale of Fig. 1). These regions of negative Φ'' are unphysical, since the spectral function must always be positive. Note that the scaling function can be written as

$$\Phi(z) = \Phi_0(z) + \frac{1}{N}\Phi_1(z) + \mathcal{O}(1/N^2) \tag{4.17}$$

The change of sign in Φ'' occurs because the $1/N$ correction Φ_1 can become dominant over the $N = \infty$ result, Φ_0, both at very low and very large z. This is an indication of the breakdown in the $1/N$ expansion at the current order
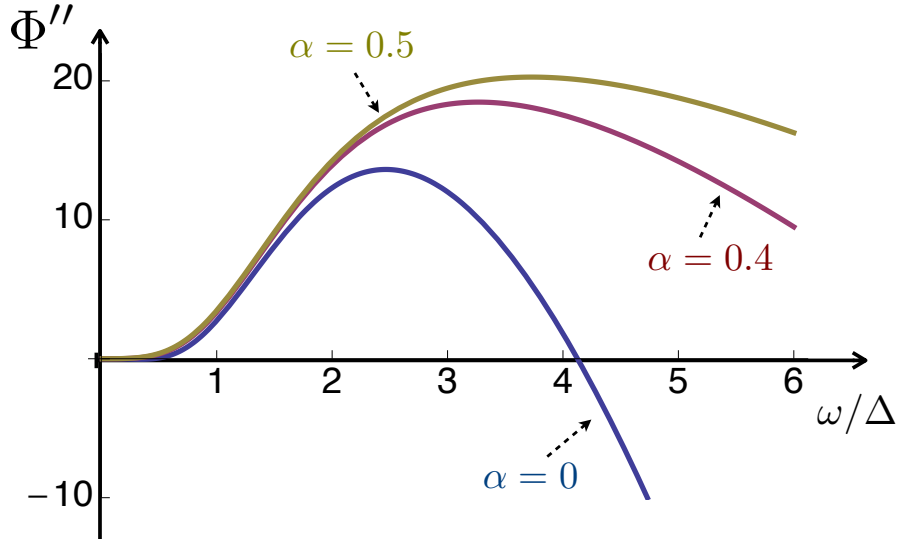
FIG. 2: Universal component of the scalar spectral function $\Phi(\omega/\Delta)$ for $N = 2$, using for $N = 2$, using the Padé approximant Eq. (4.18) for different values of α. For $\alpha = 0$, corresponding to Eq. (4.17), Φ'' becomes negative at very small and very large ω/Δ. This unphysical result is absent at $\alpha = 0.4$ and $\alpha = 0.5$.

in the case $N = 2$. One possible method to avoid the unphysical regions is to introduce a Padé approximant,

$$\Phi_{\text{Padé}}(z) = \frac{\Phi_0(z) + \frac{1-\alpha}{N}\Phi_1(z)}{1 - \frac{\alpha}{N}\Phi_1(z)/\Phi_0(z)} + \mathcal{O}(1/N^2) \tag{4.18}$$

which is equivalent to Eq. (4.17) to our working order in $1/N$. Then, by choosing an appropriate value of $\alpha \neq 0$, one obtains a positive spectral function, as shown in Fig. 2. For instance, in the small z region, Eq. (4.16) would be replaced by,

$$\mathcal{A}_{\text{Padé}} = \Lambda^{2/\nu-2}\frac{\pi^2 - 25.842(1-\alpha)/N}{1 + 25.842\alpha/(\pi^2 N)}, \tag{4.19}$$

which matches Eq. (4.16) to our working order in $1/N$, yet is positive for all values $N \geq 2$ provided $\alpha > 0.2366$.

The breakdown in the $1/N$ result in fact occurs for all N: at large enough z, Φ'' becomes negative for any N, although the value of z where this occurs increases with N. This means that there is significant ambiguity in the large-z dependence of Φ'', as seen in Fig. 2. However, many features of Φ'' are robust. For example, Φ'' displays a peak provided that the value of α is moderate. For $\alpha = 0$ the peaks in Fig. 1 are located at $\omega_{\text{peak}} \approx 2.5\Delta$ for $N = 2$, $\omega_{\text{peak}} \approx 3.5\Delta$ for $N = 3$, and $\omega_{\text{peak}} \approx 4.5\Delta$ for $N = 4$. There is uncertainty in the locations of the peaks, since these do shift when α is varied. However, the fact that the location of the peak in Φ'' is monotonically increasing with N is robust for any value of α.

B. Computation of longitudinal susceptibility

The longitudinal susceptibility $\chi(\omega)$ is related to $G_{\sigma\sigma}$ via Eq. (4.6). From scaling arguments we expect this response function to satisfy

$$G_{\sigma\sigma}^{-1}(\omega) = \Delta^{2-\eta}\Phi_\sigma(\omega/\Delta) \tag{4.20}$$

We will next compute the universal function Φ_σ to order $1/N$.

11

To order $1/N$,

$$\frac{1}{G_{\sigma\sigma}(p)} = \frac{1}{G^0_{\sigma\sigma}(p)} - \Sigma_{\sigma\sigma}(p) - \Sigma_{\lambda\lambda}(p)\frac{[G^0_{\lambda\sigma}(p)]^2}{[G^0_{\sigma\sigma}(p)]^2} - 2\Sigma_{\lambda\sigma}(p)\frac{G^0_{\lambda\sigma}(p)}{G^0_{\sigma\sigma}(p)}$$

$$= p(p + 16\sigma_0^2) + \frac{16p\sigma_0^2}{N} + \frac{8p(p + 80\sigma_0^2)}{3\pi^2 N}\ln\left(\frac{\Lambda}{16\sigma_0^2}\right)$$

$$- \frac{\sigma_0^4}{N}\left[F_{\sigma\sigma}(p) - 256F_{\lambda\lambda}(p) + 32F_{\sigma\lambda}(p)\right] \tag{4.21}$$

where the functions F are defined in Eqs. (D2-D4). Using Eq. (4.4), we find:

$$\frac{1}{G_{\sigma\sigma}(p)} = p\left(p + 4\Delta/\pi\right) + \frac{4(1-\mathcal{C})p\Delta}{\pi N} + \frac{8p(p + 4\Delta/\pi)}{3\pi^2 N}\log\left(\frac{\pi\Lambda}{4\Delta}\right)$$

$$- \frac{\Delta^2}{16\pi^2 N}\left[F_{\sigma\sigma}(p) - 256F_{\lambda\lambda}(p) + 32F_{\sigma\lambda}(p)\right]$$

$$= \Delta^2(\Delta/\Lambda)^{-\eta}H_\sigma(p/\Delta) \tag{4.22}$$

where we've used Eq. (B6) to write

$$(\Delta/\Lambda)^{-\eta} = 1 - \frac{8}{3\pi^2 N}\ln(\Delta/\Lambda) \tag{4.23}$$

and where we've introduced

$$H_\sigma(p/\Delta) = \frac{p\left(p + 4\Delta/\pi\right)}{\Delta^2} + \frac{4(1-\mathcal{C})p}{\pi N\Delta} + \frac{8p(p + 4\Delta/\pi)}{3\pi^2\Delta^2 N}\log\left(\frac{\pi}{4}\right)$$

$$- \frac{1}{16\pi^2 N}\left[F_{\sigma\sigma}(p) - 256F_{\lambda\lambda}(p) + 32F_{\sigma\lambda}(p)\right] \tag{4.24}$$

which is seen to be a universal function of p/Δ. Comparison with Eq. (4.20) gives

$$\Phi_\sigma(\omega/\Delta) = H_\sigma(-i\omega/\Delta). \tag{4.25}$$

At small values of $z = \omega/\Delta$, we can use Eq. (D5) to obtain

$$\Phi_\sigma(z) = -\left(\frac{4}{\pi} + \frac{0.5119}{N}\right)iz - \left(1 - \frac{2.2811}{N}\right)z^2$$

$$+ \left(\frac{0.2793i}{N} - \frac{24i}{9\pi N}\ln(-iz)\right)z^3 + \mathcal{O}(z^4) \tag{4.26}$$

Note the linear dependence at low z, corresponding to the infrared divergence in the longitudinal susceptibility $\chi''(\omega) \sim 1/\omega$.[3–5,7]

We compute Φ_σ numerically performing an analytic continuation as before. Figure 3 shows the imaginary part of $1/\Phi_\sigma$ for the cases $N = 2$, $N = 3$, and $N = 4$. This corresponds to the universal scaling form of $\chi''(\omega)$. In all cases, the curves are dominated by the infrared divergence $\sim 1/\omega$. In order to suppress this infrared divergence and highlight the features appearing at intermediate values of ω/Δ, we plot $\omega/\Delta \cdot \text{Im}(1/\Phi_\sigma)$ in the inset of Fig. 3 .

Equations (4.22) and (4.24) display a key feature of the longitudinal Green's function, which first appears at our current working order, $\mathcal{O}(1/N)$. For $N = \infty$, the longitudinal Green's function has poles at $p = 0$ and $p = -4\Delta/\pi$. The latter pole, which lies on the negative p axis, corresponds to an overdamped response with purely imaginary frequency $\omega = -4i\Delta/\pi$. Remarkably, at $\mathcal{O}(1/N)$, this pole acquires a real component. The appearance of a real part in ω leads to a real-time longitudinal response which has both decaying and oscillatory components.

In order to find the shift in the location of this pole, we need to solve Eq. (4.8) to order $1/N$. Equivalently, we can look for solutions to $H_\sigma(p = -4\Delta/\pi + \delta p) = 0$, where $\delta p = \mathcal{O}(1/N)$. This gives

$$\delta p = -\frac{4\Delta}{N\pi}\left\{1 - \mathcal{C} + \frac{1}{256}\left(F_{\sigma\sigma} + 32F_{\sigma\lambda} - 256F_{\lambda\lambda}\right)\right\} + \mathcal{O}(1/N^2) \tag{4.27}$$

where the functions F are to be evaluated at $p = -4\Delta/\pi$. This is carried out in Eq. (D7), where it is found
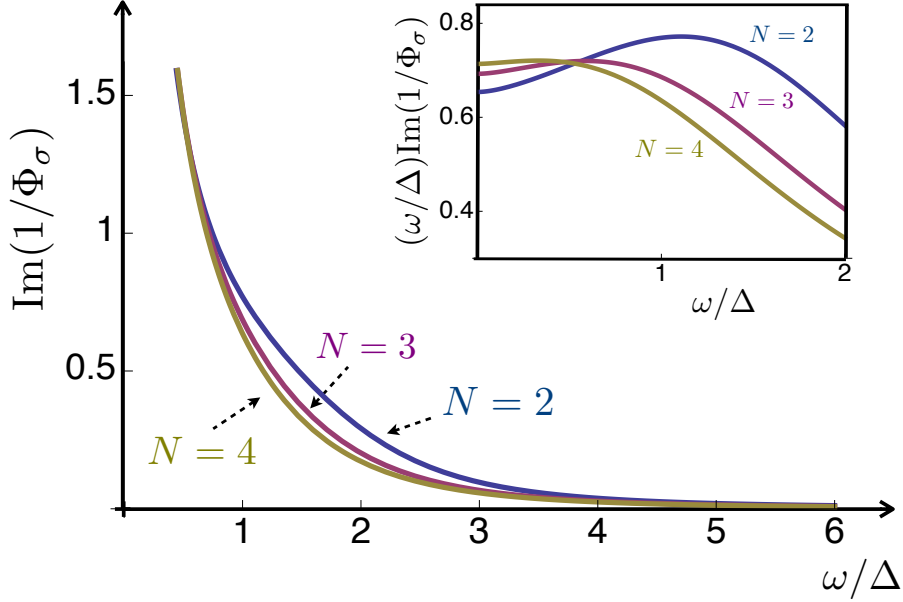
12

FIG. 3: The imaginary part of $1/\Phi_\sigma(\omega/\Delta)$, obtained from the analytic continuation of Eq. (4.24) for $N = 2$, $N = 3$, and $N = 4$. This corresponds to the universal scaling form of the longitudinal spectral function $\chi''(\omega)$. **Inset:** $\omega/\Delta \cdot \text{Im}(1/\Phi_\sigma)$, for $N = 2$, $N = 3$, and $N = 4$.

that $F_{\lambda\lambda}(-\Delta/\pi)$ has an imaginary component – this is the source of the real frequency shift in the pole, $\omega_{\text{pole}} = i(-4\Delta/\pi + \delta p)$. We find

$$\frac{\omega_{\text{pole}}}{\Delta} = -i\frac{4}{\pi} + \frac{1}{N}\left(\frac{16\left(4 + \sqrt{2}\log\left(3 - 2\sqrt{2}\right)\right)}{\pi^2} + 2.46531203396\,i\right) + \mathcal{O}(1/N^2) \tag{4.28}$$

The real part is $16\left(4 + \sqrt{2}\log\left(3 - 2\sqrt{2}\right)\right)/(N\pi^2) \sim 2.443216943237169/N$. This pole, which is most easily extracted by studying the longitudinal susceptibility, will also appear in the scalar response function $\Phi(z)$, as discussed below.

V. CONCLUSIONS

Our paper has studied the nature of Higgs excitations of the relativistic $O(N)$ model in 2+1 dimension in the Goldstone phase in the vicinity of the Wilson-Fisher fixed point.[20] It is remarkable that after nearly 40 years of study, zero temperature characteristics of this venerable fixed point have still remained uncovered.

Our main results were for the spectral function of the amplitude-squared of the order parameter which is measured in recent experiments on the superfluid-insulator quantum phase transition in Ref. 19, and in numerical simulations in Ref. 25. We expressed our results in terms of the universal complex scaling function Φ in Eq. (1.9), which measures frequency in terms of a single energy scale Δ which vanishes at the critical point with exponent ν. We obtained information on distinct features of this function: it was expanded in powers of $1/N$ in Section IV A, expanded at low frequencies in Eq. (4.15), and we determined the location of the pole in the lower-half complex frequency plane in Section IV B. The pole is specified in Eq. 1.5: note that both its real and imaginary parts are proportional to Δ, and so the width of the Higgs particle is of the same order as its energy.

Here we combine these results to obtain useful interpolating forms for comparing with numerical or experimental data. We consider Φ as function of the complex variable $z = \omega/\Delta = ip/\Delta$. An explicit form with all the necessary analytic features is

$$\Phi(z) = \frac{z^2}{1 + ic_1 z + c_2 z^2 + ic_3 z^3 + ic_4 z^3 \ln(-iz)} + c_0 \tag{5.1}$$

where $c_{0,1,2,3,4}$ are real constants. The constraints on these constants are:
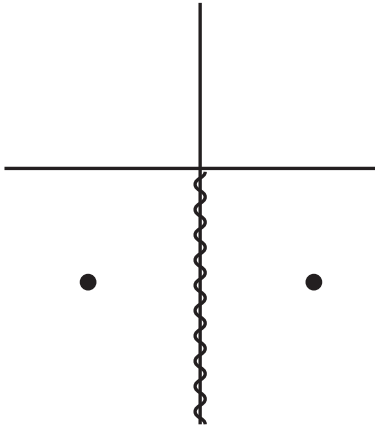
13

FIG. 4: Analytic structure of the *retarded* Green's function $\Phi(z)$ in Eq. (5.1). This is analytic and unique in the upper-half plane, but its structure in the lower-half plane depends upon the choice of a branch-cut originating at $z = 0$. If we analytically continue from the upper-half plane, we find a pole in the lower-half plane, but its location depends upon the manner in which we encircle $z = 0$. The figure shows the choice of the branch-cut along the negative imaginary axis. Then the pole is at Eq. (4.28) or at the partner point with the opposite sign for the real part. Note the similarity to the analytic structure of the strongly coupled gapless systems studied using the AdS/CFT correspondence in Refs. 27–29.

- $\Phi(z)$ is real on the imaginary axis in the upper-half plane, $z = ip/\Delta$ with $p > 0$.

- $\Phi(z)$ is analytic in the upper-half plane.

- There is a branch cut in $\Phi(z)$ starting from $z = 0$, we take this cut to lie in the lower-half plane. Upon analytically continuing $\Phi(z)$ clockwise from the imaginary axis in the upper-half plane we find a single pole in the lower-half plane. The position of this pole should coincide with Eq. (1.5). On the other hand, if we analytically continue $\Phi(z)$ anticlockwise from the upper-half plane we again find only a single pole in the lower-half plane, but its real part has changed sign. One convenient choice is to place the branch cut along the lower imaginary axis, leading to the analytic structure shown in Fig. 4. This analytic structure is remarkably similar to that found in recent studies using the AdS/CFT correspondence.[27–29] These studies describe a particle interacting strongly with a gapless continuum of excitations, and so bears a similarity to our study of the Higgs particle interacting strongly with the Goldstone excitations.

- The small z expansion of $\Phi(z)$ should agree with Eq. (4.15).

In addition, we expect $\Phi(z) \sim z^{3-2/\nu}$ in the limit $z \gg 1$, as required in order to ensure that $S(\omega)$ is independent of Δ when $\omega \gg \Delta$. Equation (5.1) does not satisfy this requirement. However, a comparison with experiments or with numerical simulations is bound to be complicated at high-frequencies by lattice-scale contributions. Thus, we choose to focus on the regime in which the frequency is not much greater than Δ. Then Eq. (5.1) can serve as a useful prototypical form to fit the data.

Finally, we note that the scaling function $\Phi_\sigma(z)$, which specifies the response function $\chi(\omega)$ via Eq. (4.20), has a very similar analytic structure. The only change from $\Phi(z)$ is that there is an additional pole at $z = 0$. However the locations of the poles in the lower-half plane are the same, and there is also a branch cut starting at $z = 0$.

Appendix A: Nonlinear terms in action

This appendix will specify the non-linear terms, $\mathcal{S}_1$, in the functional integral over λ in Eq. (2.4). They are given by

$$
\mathcal{S}_1 = -\frac{i}{6\sqrt{N}} \int_{\boldsymbol{p}_1, \boldsymbol{p}_2, \boldsymbol{p}_3} K_3(\boldsymbol{p}_1, \boldsymbol{p}_2, \boldsymbol{p}_3) \lambda(\boldsymbol{p}_1)\lambda(\boldsymbol{p}_2)\lambda(\boldsymbol{p}_3)\, \delta\left(\sum_{i=1}^{3} \boldsymbol{p}_i\right)
$$
$$
- \frac{1}{24N} \int_{\boldsymbol{p}_1, \boldsymbol{p}_2, \boldsymbol{p}_3, \boldsymbol{p}_4} K_4(\boldsymbol{p}_1, \boldsymbol{p}_2, \boldsymbol{p}_3, \boldsymbol{p}_4) \lambda(\boldsymbol{p}_1)\lambda(\boldsymbol{p}_2)\lambda(\boldsymbol{p}_3)\lambda(\boldsymbol{p}_4)\, \delta\left(\sum_{i=1}^{4} \boldsymbol{p}_i\right). \tag{A1}
$$

The three-point vertex is given by[30]

$$
\begin{aligned}
K_3(\boldsymbol{p}_1, \boldsymbol{p}_2, \boldsymbol{p}_3) &= \int_{\boldsymbol{q}} \frac{1}{(q^2+r)((\boldsymbol{q}+\boldsymbol{p}_1)^2+r)((\boldsymbol{q}-\boldsymbol{p}_2)^2+r)} \\
&= \frac{1}{4\pi P} \tan^{-1} \frac{P}{\sqrt{r(p_1^2+p_2^2+p_3^2+8r)}} \\
&\equiv K_3(p_1, p_2, p_3),
\end{aligned} \tag{A2}
$$

where

$$
P^2 = p_1^2 p_2^2 p_3^2 + r(p_1^2+p_2^2+p_3^2)^2 - 2r(p_1^4+p_2^4+p_3^4). \tag{A3}
$$

At the critical point, with $r \to 0$, we have

$$
K_3(p_1, p_2, p_3) = \frac{1}{8 p_1 p_2 p_3}. \tag{A4}
$$

At the critical point, we will also need

$$
\begin{aligned}
K_3(\boldsymbol{p}, -\boldsymbol{p}, 0) &= \frac{\Pi(0,0)}{p^2} + \int_{\boldsymbol{q}} \frac{1}{q^4}\left(\frac{1}{(\boldsymbol{q}+\boldsymbol{p})^2} - \frac{1}{p^2}\right) \\
&= \frac{\Pi(0,0)}{p^2}.
\end{aligned} \tag{A5}
$$

where we have used the curious fact that

$$
\int_{\boldsymbol{p}} \frac{1}{p^4}\left(\frac{1}{(\boldsymbol{p}+\boldsymbol{q})^2} - \frac{1}{q^2}\right) = 0 \tag{A6}
$$

only in 3 spacetime dimensions. Similarly, the 4-point vertex is

$$
K_4(\boldsymbol{p}_1, \boldsymbol{p}_2, \boldsymbol{p}_3, \boldsymbol{p}_4) = 3 \int_{\boldsymbol{q}} \frac{1}{(q^2+r)((\boldsymbol{q}+\boldsymbol{p}_1)^2+r)((\boldsymbol{q}+\boldsymbol{p}_1+\boldsymbol{p}_2)^2+r)((\boldsymbol{q}-\boldsymbol{p}_4)^2+r)}. \tag{A7}
$$

We will not need this expression in general, but only 2 special cases; we have

$$
\begin{aligned}
K_4(\boldsymbol{p}, \boldsymbol{k}, -\boldsymbol{p}, -\boldsymbol{k}) &= 3 \int_{\boldsymbol{q}} \frac{1}{(q^2+r)((\boldsymbol{q}+\boldsymbol{p})^2+r)((\boldsymbol{q}+\boldsymbol{p}+\boldsymbol{k})^2+r)((\boldsymbol{q}+\boldsymbol{k})^2+r)} \\
&= \frac{3}{2(\boldsymbol{p}\cdot\boldsymbol{k})} \int_{\boldsymbol{q}} \frac{q^2+r+(\boldsymbol{q}+\boldsymbol{p}+\boldsymbol{k})^2+r-(\boldsymbol{q}+\boldsymbol{p})^2-r-(\boldsymbol{q}+\boldsymbol{k})^2-r}{(q^2+r)((\boldsymbol{q}+\boldsymbol{p})^2+r)((\boldsymbol{q}+\boldsymbol{p}+\boldsymbol{k})^2+r)((\boldsymbol{q}+\boldsymbol{k})^2+r)} \\
&= \frac{3}{(\boldsymbol{p}\cdot\boldsymbol{k})} \left[K_3(k, p, |\boldsymbol{k}-\boldsymbol{p}|) - K_3(k, p, |\boldsymbol{k}+\boldsymbol{p}|)\right],
\end{aligned} \tag{A8}
$$

and from Ref. 31 at the critical point

$$K_4(\boldsymbol{p}, -\boldsymbol{p}, \boldsymbol{k}, -\boldsymbol{k}) = 3 \int_{\boldsymbol{q}} \frac{1}{q^4(\boldsymbol{q} + \boldsymbol{p})^2(\boldsymbol{q} + \boldsymbol{k})^2}$$

$$= 3\frac{\Pi(0,0)}{p^2 k^2} + 3\int_{\boldsymbol{q}} \frac{1}{q^4} \left(\frac{1}{(\boldsymbol{q} + \boldsymbol{p})^2(\boldsymbol{q} + \boldsymbol{k})^2} - \frac{1}{p^2 k^2} \right)$$

$$= 3\frac{\Pi(0,0)}{p^2 k^2} + \frac{3(\boldsymbol{p} \cdot \boldsymbol{k})}{8p^3 k^3 |\boldsymbol{p} - \boldsymbol{k}|}. \tag{A9}$$

Appendix B: Critical singularities

This appendix will review the derivation of the quantum critical singularities at $g = g_c$ using the basic expressions in Section II. We will set $u = \infty$ in all expressions here.

Let us first determine the value of the critical coupling g_c to order $1/N$. The critical point is determined by the condition $G^{-1}(0) = 0$. So at the critical point $r = r_c$ where, from Eq. (2.11),

$$r_c = -\frac{2}{N} \int_{\boldsymbol{q}} \frac{1}{\Pi(q,0)} \frac{1}{q^2} + \frac{2}{N} \frac{1}{\Pi(0,0)} \int_{\boldsymbol{p},\boldsymbol{q}} \frac{1}{p^4(\boldsymbol{p} + \boldsymbol{q})^2} \frac{1}{\Pi(q,0)}$$

$$= \frac{2}{N} \frac{1}{\Pi(0,0)} \int_{\boldsymbol{q}} \frac{1}{\Pi(q,0)} \int_{\boldsymbol{p}} \frac{1}{p^4} \left(\frac{1}{(\boldsymbol{p} + \boldsymbol{q})^2} - \frac{1}{q^2} \right) \tag{B1}$$

Note that $\Pi(0,0)$ is infrared divergent, but we assume this is suitably regulated by putting the theory in finite box; we will find that $\Pi(0,0)$ will eventually cancel out. Using Eq. (A6), we conclude that

$$r_c = \mathcal{O}(1/N^2). \tag{B2}$$

So from Eq. (2.3), we obtain

$$\frac{1}{g_c} = \int_{\boldsymbol{p}} \frac{1}{p^2} + \mathcal{O}(1/N^2). \tag{B3}$$

Next, we determine the exponent η. For this we need $G^{-1}(p)$ at the critical point $r = r_c$. This is given by

$$G^{-1}(p) = p^2 + \frac{2}{N} \int_{\boldsymbol{q}} \frac{1}{\Pi(q,0)} \left(\frac{1}{(\boldsymbol{p} + \boldsymbol{q})^2} - \frac{1}{q^2} \right) \tag{B4}$$

We have

$$G^{-1}(p)) = p^2 \left(1 + \eta \ln \left(\frac{\Lambda}{p} \right) \right) \tag{B5}$$

where

$$\eta = \frac{8}{3\pi^2 N}. \tag{B6}$$

For the exponent, ν, assume the coupling is g, and define r_g by

$$\frac{1}{g_c} - \frac{1}{g} \equiv \int_{\boldsymbol{p}} \left(\frac{1}{p^2} - \frac{1}{p^2 + r_g} \right)$$

$$\equiv \frac{\sqrt{r_g}}{4\pi}. \tag{B7}$$

Then from Eq. (2.3) and (B3) we have

$$r = r_g + \mathcal{O}(1/N^2). \tag{B8}$$

16

Now combining Eq. (2.11) and (B8), we have the result for the inverse susceptibility

$$G^{-1}(p) = p^2 + r + F(p, r) \tag{B9}$$

where

$$F(p, r) = \frac{2}{N} \int_{\boldsymbol{q}} \frac{1}{\Pi(q, r)} \left[\frac{1}{((\boldsymbol{p} + \boldsymbol{q})^2 + r)} + \frac{\Pi'(q, r)}{2\Pi(0, r)} \right], \tag{B10}$$

with

$$\Pi'(p, r) \equiv \frac{\partial \Pi(p, r)}{\partial r} = -2 \int_{\boldsymbol{q}} \frac{1}{(q^2 + r)^2 ((\boldsymbol{p} + \boldsymbol{q})^2 + r)} = -\frac{1}{4\pi\sqrt{r}(p^2 + 4r)}. \tag{B11}$$

A useful check is to note that $G^{-1}(0) = 0$ as $r \to 0$. From (B10) we have

$$\begin{aligned}
F(0, r) &= \frac{12r}{N\pi} \int_0^\Lambda dq \frac{q^3}{(q^2 + r)(q^2 + 4r)\tan^{-1}(q/(2\sqrt{r}))} \\
&\approx \frac{12}{N\pi^2} r \ln\left(\frac{\Lambda^2}{r}\right)
\end{aligned} \tag{B12}$$

From this we obtain the exponent

$$\gamma = 2 - \frac{24}{N\pi^2}. \tag{B13}$$

Let us now obtain the connected Green's function, $G_{\lambda\lambda}(p)$ to order $1/N$ at the critical point $r = r_c$. We insert (A4,A5,A8,A9) into (2.8,2.10). All occurrences of $\Pi(0, 0)$ cancel out, and

$$\begin{aligned}
G_{\lambda\lambda}(p) &= 16p - \frac{512}{N} \int_{\boldsymbol{k}} \frac{1}{k|\boldsymbol{k} - \boldsymbol{p}|} + \frac{256p}{N} \int_{\boldsymbol{k}} \frac{1}{(\boldsymbol{p} \cdot \boldsymbol{k})} \left[\frac{1}{|\boldsymbol{k} - \boldsymbol{p}|} - \frac{1}{|\boldsymbol{k} + \boldsymbol{p}|} \right] + \frac{512}{N} \int_{\boldsymbol{k}} \frac{(\boldsymbol{p} \cdot \boldsymbol{k})}{pk^2|\boldsymbol{p} - \boldsymbol{k}|} \\
&= 16p - \frac{128}{N\pi^2}(2\Lambda - p) + \frac{256p}{N\pi^2} \ln\left(\frac{\Lambda}{p}\right) + \frac{256p}{3N\pi^2}\left(\ln\left(\frac{\Lambda}{p}\right) + \frac{1}{3}\right) \\
&= -\frac{256\Lambda}{N\pi^2} + 16p\left(1 + \frac{64}{3\pi^2 N} \ln\left(\frac{\Lambda}{p}\right) + \frac{22}{3}\right)
\end{aligned} \tag{B14}$$

The scaling dimension of λ is the same as that of ϕ_α^2, which is $3 - 1/\nu$, and so we expect

$$G_{\lambda\lambda}(p) \sim \text{constant} + p^{3 - 2/\nu} \tag{B15}$$

and so (B14) is consistent with (3.4).

Appendix C: Computation of threshold singularity

We describe the evaluation of the $\boldsymbol{k}$ integral in Eq. (3.8) at $p = -i(2\Delta + \omega)$ as $\omega \to 0$.

The singularities arising from the integral of $\boldsymbol{k}$ in Eq. (3.8) are all at energy 4Δ, and so we only need the explicit

singularities of all the terms as $p \to -i(2\sqrt{r} + \omega)$. We list these:

$$\Pi(p, r) = \frac{1}{16\pi\sqrt{r}} \ln\left(\frac{4\sqrt{r}}{-\omega}\right)$$

$$\Pi(|\boldsymbol{p}+\boldsymbol{k}|, r) = \frac{1}{16\pi\sqrt{r}(1 + ikx/\sqrt{r} - k^2/(4r))^{1/2}} \ln\left(\frac{1 + (1 + ikx/\sqrt{r} - k^2/(4r))^{1/2}}{1 - (1 + ikx/\sqrt{r} - k^2/(4r))^{1/2}}\right)$$

$$K_3(p, k, |\boldsymbol{p}+\boldsymbol{k}|) = \frac{1}{16\pi\sqrt{r}k(k - 2i\sqrt{r}x)} \left[\ln\left(\frac{4\sqrt{r}}{-\omega}\right) + \ln\left(\frac{k\sqrt{r}(k - 2i\sqrt{r}x)^2}{(k^2 + 4r)(k - 4i\sqrt{r}x)}\right)\right]$$

$$K_4(\boldsymbol{p}, \boldsymbol{k}, -\boldsymbol{p}, -\boldsymbol{k}) = \frac{3}{16\pi r k^2 x} \mathrm{Im}\left\{\frac{1}{(k - 2i\sqrt{r}x + (k^2 - 6ik\sqrt{r}x - 4r(1 + x^2))\omega/(2\sqrt{r}(k - 2i\sqrt{r}x)))}\right.$$
$$\left. \times \left[\ln\left(\frac{4\sqrt{r}}{-\omega}\right) + \ln\left(\frac{k\sqrt{r}(k - 2i\sqrt{r}x)^2}{(k^2 + 4r)(k - 4i\sqrt{r}x)}\right)\right]\right\} \tag{C1}$$

where $x \equiv (\boldsymbol{p} \cdot \boldsymbol{k})/(pk)$.

For the second term in Eq. (3.8), we can now pick out the co-efficient of the threshold singularity to be

$$-\frac{8}{\pi^2 N}\left[\ln\left(\frac{4\sqrt{r}}{-\omega}\right)\right]^{-1} \frac{1}{2} \int_{-1}^{1} dx \int_{0}^{\infty} dk \ln\left(\frac{k\sqrt{r}(k - 2i\sqrt{r}x)^2}{(k^2 + 4r)(k - 4i\sqrt{r}x)}\right) \frac{1}{(k - 2i\sqrt{r}x)^2 \Pi(|\boldsymbol{k}+\boldsymbol{p}|, r)\Pi(k, r)}$$
$$= \frac{32\pi\sqrt{r}}{N}\left[\ln\left(\frac{4\sqrt{r}}{-\omega}\right)\right]^{-1} \times 4.507333003 \tag{C2}$$

For the last term in Eq. (3.8), the term associated with the explicit $\ln(4\sqrt{r}/(-\omega))$ term in K_4 is

$$\frac{1}{N}\left[\ln\left(\frac{4\sqrt{r}}{-\omega}\right)\right]^{-1} \frac{1}{2} \int_{-1}^{1} dx \int_{0}^{\Lambda} dk \frac{128k}{x \tan^{-1}(k/(2\sqrt{r}))}$$
$$\times \mathrm{Im}\left\{\frac{1}{(k - 2i\sqrt{r}x + (k^2 - 6ik\sqrt{r}x - 4r(1 + x^2))\omega/(2\sqrt{r}(k - 2i\sqrt{r}x)))}\right\}$$
$$= \frac{32\pi\sqrt{r}}{N}\left[\ln\left(\frac{4\sqrt{r}}{-\omega}\right)\right]^{-1}\left\{2\ln\left(\frac{4\sqrt{r}}{-\omega}\right) + \frac{16}{\pi^2}\ln\left(\frac{\Lambda}{\sqrt{r}}\right) - 3.44906254\right\} \tag{C3}$$

The $\ln(\Lambda)$ term above has the same co-efficient as that expected from the corresponding term in Eq. (B14).

The remaining contribution of the last term in Eq. (3.8) is

$$\frac{1}{N}\left[\ln\left(\frac{4\sqrt{r}}{-\omega}\right)\right]^{-2} \frac{1}{2} \int_{-1}^{1} dx \int_{0}^{\infty} dk \frac{128k}{x \tan^{-1}(k/(2\sqrt{r}))} \ln\left(\frac{k\sqrt{r}(k - 2i\sqrt{r}x)^2}{(k^2 + 4r)(k - 4i\sqrt{r}x)}\right)$$
$$\times \mathrm{Im}\left\{\frac{1}{(k - 2i\sqrt{r}x + (k^2 - 6ik\sqrt{r}x - 4r(1 + x^2))\omega/(2\sqrt{r}(k - 2i\sqrt{r}x)))}\right\}$$
$$= \frac{32\pi\sqrt{r}}{N}\left[\ln\left(\frac{4\sqrt{r}}{-\omega}\right)\right]^{-1}\left\{-\ln\left(\frac{4\sqrt{r}}{-\omega}\right) + 1.3863\right\} \tag{C4}$$

Putting the contributions to the last term of Eq. (3.8) in Eqs. (C3,C4) together, we have

$$\frac{4}{3\Pi^2(p, r)} \int_{\boldsymbol{k}} \frac{K_4(\boldsymbol{p}, \boldsymbol{k}, -\boldsymbol{p}, -\boldsymbol{k})}{\Pi(k, r)} =$$
$$32\pi\sqrt{r}\left\{1 + \left[\ln\left(\frac{4\sqrt{r}}{-\omega}\right)\right]^{-1}\left(\frac{16}{\pi^2}\ln\left(\frac{\Lambda}{\sqrt{r}}\right) - 2.063\right)\right\} \tag{C5}$$

Inserting the results in Eqs. (3.5, C2, C5) into Eq. (3.8), we obtain Eq. (3.9).

Appendix D: Self energies in the Goldstone phase

We can compute the self-energies associated with the bare connected Green's functions in Eq. (4.7) by a standard $1/N$ expansion of the partition function in Eq. (4.5). The self-energies to order $1/N$ are

$$
\begin{aligned}
\Sigma_{\sigma\sigma}(p) &= -\frac{1}{N}\int_{\boldsymbol{k}} G^0_{\sigma\sigma}(|\boldsymbol{k}+\boldsymbol{p}|)G^0_{\lambda\lambda}(k) - \frac{1}{N}\int_{\boldsymbol{k}} G^0_{\sigma\lambda}(|\boldsymbol{k}+\boldsymbol{p}|)G^0_{\sigma\lambda}(k) - \frac{1}{N}G^0_{\sigma\lambda}(0)\int_{\boldsymbol{k}} G^0_{\sigma\lambda}(k) \\
&= \frac{256\sigma_0^2\Lambda}{\pi^2 N} - \frac{8(p^2+3072\sigma_0^4)}{3\pi^2 N}\ln\left(\frac{\Lambda}{16\sigma_0^2}\right) + \frac{\sigma_0^4}{N}F_{\sigma\sigma}(p) \\[4pt]
\Sigma_{\lambda\lambda}(p) &= \frac{1}{2N}\Pi(p,0) - \frac{1}{2N}\int_{\boldsymbol{k}} G^0_{\sigma\sigma}(|\boldsymbol{k}+\boldsymbol{p}|)G^0_{\sigma\sigma}(k) - \frac{1}{2N}\int_{\boldsymbol{k}} \left[K_3(\boldsymbol{p},\boldsymbol{k},-\boldsymbol{p}-\boldsymbol{k})\right]^2 G^0_{\lambda\lambda}(|\boldsymbol{k}+\boldsymbol{p}|)G^0_{\lambda\lambda}(k) \\
&\quad + \frac{1}{N}\int_{\boldsymbol{k}} K_3(\boldsymbol{p},\boldsymbol{k},-\boldsymbol{p}-\boldsymbol{k})G^0_{\sigma\lambda}(|\boldsymbol{k}+\boldsymbol{p}|)G^0_{\sigma\lambda}(k) + \frac{1}{N}K_3(\boldsymbol{p},-\boldsymbol{p},0)G^0_{\sigma\lambda}(0)\int_{\boldsymbol{k}} G^0_{\sigma\lambda}(k) \\
&\quad + \frac{1}{6N}\int_{\boldsymbol{k}} K_4(\boldsymbol{p},\boldsymbol{k},-\boldsymbol{p},-\boldsymbol{k})G^0_{\lambda\lambda}(k) + \frac{1}{3N}\int_{\boldsymbol{k}} K_4(\boldsymbol{p},-\boldsymbol{p},\boldsymbol{k},-\boldsymbol{k})G^0_{\lambda\lambda}(k) \\
&= -\frac{\Lambda}{\pi^2 N p^2} + \frac{4(p+24\sigma_0^2)}{3\pi^2 N p^2}\ln\left(\frac{\Lambda}{16\sigma_0^2}\right) + \frac{1}{16Np} + \frac{\sigma_0^2}{Np^2}F_{\lambda\lambda}(p) \\[4pt]
\Sigma_{\sigma\lambda}(p) &= -\frac{1}{N}\int_{\boldsymbol{k}} G^0_{\sigma\sigma}(|\boldsymbol{k}+\boldsymbol{p}|)G^0_{\sigma\lambda}(k) + \frac{1}{N}\int_{\boldsymbol{k}} K_3(\boldsymbol{p},\boldsymbol{k},-\boldsymbol{p}-\boldsymbol{k})G^0_{\sigma\lambda}(|\boldsymbol{k}+\boldsymbol{p}|)G^0_{\lambda\lambda}(k) \\
&\quad - \frac{1}{N}G^0_{\sigma\sigma}(0)\int_{\boldsymbol{k}} G^0_{\sigma\lambda}(k) - \frac{1}{2N}G^0_{\sigma\lambda}(0)\int_{\boldsymbol{k}} G^0_{\sigma\sigma}(k) \\
&\quad + \frac{1}{2N}G^0_{\sigma\lambda}(0)\int_{\boldsymbol{k}} K_3(\boldsymbol{k},-\boldsymbol{k},0)G^0_{\lambda\lambda}(k) + \frac{1}{2N}G^0_{\sigma\lambda}(0)\int_{\boldsymbol{k}} \frac{1}{k^2} \\
&= -\frac{16i\sigma_0\Lambda}{\pi^2 N p} + \frac{4i\sigma_0(p+128\sigma_0^2)}{\pi^2 N p}\ln\left(\frac{\Lambda}{16\sigma_0^2}\right) + \frac{i\sigma_0^3}{Np}F_{\sigma\lambda}(p)
\end{aligned}
\tag{D1}
$$

Note that all the terms involving $\Pi(0,0)$ in Eq. (D1) do indeed cancel with each other. In the last line of each expression in Eq. (D1) we have extracted the ultraviolet divergences explicitly; the functions F are finite and universal dimensionless functions, which depend only on the ratio p/σ_0^2. They are given by the integrals:

$$
\begin{aligned}
F_{\sigma\sigma}(p) &= \frac{1}{\sigma_0^4}\int_{\boldsymbol{k}}\left[\frac{k^2+256\sigma_0^4}{\sigma_0^2(k+16\sigma_0^2)(|\boldsymbol{k}+\boldsymbol{p}|+16\sigma_0^2)} - \frac{k^2}{\sigma_0^2|\boldsymbol{k}+\boldsymbol{p}|(k+16\sigma_0^2)} + \frac{16}{k+16\sigma_0^2} \right. \\
&\qquad\qquad\left. - \frac{512\sigma_0^2}{k^2} + \frac{16(p^2+3072\sigma_0^4)}{3k^2(k+16\sigma_0^2)}\right] \\
&= -\int_0^p dk\, \frac{8\left(-3k^2(p+16\sigma_0^2)+3\left(k^2+256\sigma_0^4\right)k\tanh^{-1}\left(\frac{k}{p+16\sigma_0^2}\right)+96kp\sigma_0^2-p\left(p^2+1536\sigma_0^2\right)\right)}{3\pi^2\sigma_0^4(k+16\sigma_0^2)p} \\
&\quad - \int_p^\infty dk\, \frac{8\left(3k\left(k^2+256\sigma_0^4\right)\tanh^{-1}\left(\frac{p}{k+16\sigma_0^2}\right)-p\left(3k^2-48k\sigma_0^2+p^2+1536\sigma_0^4\right)\right)}{3\pi^2\sigma_0^4(k+16\sigma_0^2)p}
\end{aligned}
\tag{D2}
$$

$$F_{\lambda\lambda}(p) = \frac{p^2}{\sigma_0^2} \int_{\boldsymbol{k}} \left[\frac{k(|\boldsymbol{k}+\boldsymbol{p}| - |\boldsymbol{k}-\boldsymbol{p}|)}{p(\boldsymbol{p}\cdot\boldsymbol{k})|\boldsymbol{k}+\boldsymbol{p}||\boldsymbol{k}-\boldsymbol{p}|(k+16\sigma_0^2)} + \frac{2(\boldsymbol{p}\cdot\boldsymbol{k})}{kp^3|\boldsymbol{k}-\boldsymbol{p}|(k+16\sigma_0^2)} \right.$$

$$+ \frac{p^2 - 64k\sigma_0^2 + 64p\sigma_0^2}{32kp^2\sigma_0^2(k+16\sigma_0^2)(|\boldsymbol{k}+\boldsymbol{p}|+16\sigma_0^2)} - \frac{p+64\sigma_0^2}{32kp\sigma_0^2|\boldsymbol{k}+\boldsymbol{p}|(k+16\sigma_0^2)} + \frac{2}{k^2p^2} - \frac{8(p+24\sigma_0^2)}{3p^2k^2(k+16\sigma_0^2)} \right]$$

$$= \int_0^p dk \left[\frac{k^2 \log\left(\frac{2k\left(\sqrt{k^2+p^2}+k\right)+p^2}{p^2}\right)}{2\pi^2\sigma_0^2(k+16\sigma_0^2)\sqrt{k^2+p^2}} + \frac{(64k\sigma_0^2 - p^2 - 64p\sigma_0^2)\tanh^{-1}\left(\frac{k}{p+16\sigma_0^2}\right)}{4\pi^2\sigma_0^2(k+16\sigma_0^2)p} \right.$$

$$\left. + \frac{4k^3 - 12k^2p + 12kp^2 - 16p^3 - 192p^2\sigma_0^2}{12\pi^2\sigma_0^2(k+16\sigma_0^2)p^2} \right]$$

$$+ \int_p^\infty dk \left[\frac{k^2 \log\left(\frac{k^2+2p\left(\sqrt{k^2+p^2}+p\right)}{k^2}\right)}{2\pi^2\sigma_0^2(k+16\sigma_0^2)\sqrt{k^2+p^2}} + \frac{(64k\sigma_0^2 - p^2 - 64p\sigma_0^2)\tanh^{-1}\left(\frac{p}{k+16\sigma_0^2}\right)}{4\pi^2\sigma_0^2(k+16\sigma_0^2)p} \right.$$

$$\left. - \frac{p+16\sigma_0^2}{\pi^2\sigma_0^2(k+16\sigma_0^2)} \right] \tag{D3}$$

$$F_{\sigma\lambda}(p) = \frac{1}{\sigma_0^2} \int_{\boldsymbol{k}} \left[\frac{2k-p}{\sigma_0^2(k+16\sigma_0^2)(|\boldsymbol{k}+\boldsymbol{p}|+16\sigma_0^2)} - \frac{2k-p}{\sigma_0^2|\boldsymbol{k}+\boldsymbol{p}|(k+16\sigma_0^2)} - \frac{8p}{k^2(k+16\sigma_0^2)} \right.$$

$$\left. + \frac{32}{k^2} - \frac{8(p+128\sigma_0^2)}{k^2(k+16\sigma_0^2)} \right]$$

$$= -\int_0^p dk \frac{8\left(p(-2k+p+32\sigma_0^2) + k(2k-p)\tanh^{-1}\left(\frac{k}{p+16\sigma_0^2}\right)\right)}{\pi^2\sigma_0^2(k+16\sigma_0^2)p}$$

$$- \int_p^\infty dk \frac{8\left(p(-2k+p+32\sigma_0^2) + k(2k-p)\tanh^{-1}\left(\frac{p}{k+16\sigma_0^2}\right)\right)}{\pi^2\sigma_0^2(k+16\sigma_0^2)p} \tag{D4}$$

At small values of p we find

$$F_{\sigma\sigma}(p) = \frac{4096}{\pi^2} + \frac{40p^2}{9\pi^2\sigma_0^4} + \frac{7p^4}{4800\pi^2\sigma_0^8} - \frac{7p^5}{92160\pi^2\sigma_0^{1}0} + \frac{17p^6}{4816896\pi^2\sigma_0^{12}} + \mathcal{O}(p^7),$$

$$F_{\sigma\lambda}(p) = -\frac{256}{\pi^2} - \frac{8p}{\pi^2\sigma_0^2} - \frac{p^2}{9\pi^2\sigma_0^4} + \frac{p^3}{576\pi^2\sigma_0^6} - \frac{3p^4}{5120\pi^2\sigma_0^8} + \frac{19p^5}{7372800\pi^2\sigma_0^{10}} + \mathcal{O}(p^6), \tag{D5}$$

$$F_{\lambda\lambda}(p) = -\frac{16}{\pi^2} - \frac{p}{\pi^2\sigma_0^2} - 0.0083038708178\frac{p^2}{\sigma_0^4} + 0.00077664324643133\frac{p^3}{\sigma_0^6}$$

$$+ 0.000022616797187123\frac{p^4}{\sigma_0^8} - 2.34860390339644 \times 10^{-6}\frac{p^5}{\sigma_0^{10}} + \mathcal{O}(p^6)$$

$$+ \left(-\frac{p^3}{384\pi^2\sigma_0^6} + \frac{p^5}{122880\pi^2\sigma_0^{10}} + \mathcal{O}(p^7) \right) \log(p/\sigma_0^2), \tag{D6}$$

whereas for general values of p these functions can be evaluated numerically. Notice that the $\log(p)$ terms are present only in $F_{\lambda\lambda}$, and these arise from the integral of the explicitly displayed logarithm in Eq. (D3).

The imaginary parts of these functions at $p = -16\sigma_0^2$ are obtained by analytically continuing the contour integration

via $k \to ke^{i\theta}$, $p \to pe^{i\theta}$ and then taking the limit $\theta \searrow -\pi$.

$$\lim_{\theta \searrow -\pi} \operatorname{Im} F_{\sigma\sigma}(16\sigma_0^2 e^{i\theta}) = -\int_0^{-32\sigma_0^2} \frac{kdk}{4\pi\sigma_0^6}(k^2 + 256\sigma_0^4)\,\mathcal{P}\left(\frac{1}{k+16\sigma_0^2}\right) - \frac{26624}{3\pi} = 0$$

$$\lim_{\theta \searrow -\pi} \operatorname{Im} F_{\sigma\lambda}(16\sigma_0^2 e^{i\theta}) = -\int_0^{-32\sigma_0^2} \frac{kdk}{2\pi\sigma_0^4}(k + 8\sigma_0^2)\,\mathcal{P}\left(\frac{1}{k+16\sigma_0^2}\right) + \frac{384}{\pi} = 0$$

$$\lim_{\theta \searrow -\pi} \operatorname{Im} F_{\lambda\lambda}(-16\sigma_0^2 e^{i\theta}) = \int_0^{-32\sigma_0^2} \frac{dk}{2\pi\sigma_0^2}(k + 12\sigma_0^2)\,\mathcal{P}\left(\frac{1}{k+16\sigma_0^2}\right) - \frac{(4\sqrt{2}\ln(3 - 2\sqrt{2}))}{\pi}$$

$$= -\frac{(16 + 4\sqrt{2}\ln(3 - 2\sqrt{2}))}{\pi} \tag{D7}$$

The numerical values of these functions evaluated by Mathematica at a series of values of θ starting at $\theta = 0$, and converging to $\theta = -\pi$, lead to

$$F_{\sigma\sigma}(-16\sigma_0^2) = 585.93223 + 5 \times 10^{-7}\,i$$
$$F_{\sigma\lambda}(-16\sigma_0^2) = -19.0308885 + 3 \times 10^{-8}\,i$$
$$F_{\lambda\lambda}(-16\sigma_0^2) = -1.5589876 - 1.9188981\,i, \tag{D8}$$

in excellent agreement with the values in Eq. (D7). Note that the imaginary values are restricted to $F_{\lambda\lambda}$, and it is this imaginary contribution which leads to the real part of the pole in Eq. (1.5). This imaginary value of $F_{\lambda\lambda}$ is again a consequence of the explicitly displayed logarithm in Eq. (D3). Thus the $\log(p)$ terms in Eq. (D6) and the oscillatory component of the pole are linked to each other, as is also noted in Section V.

[1] S. Chakravarty, B.I. Halperin, and D.R. Nelson, Phys. Rev. Lett. **60**, 1057 (1988).

[2] M. P. A. Fisher, P. B. Weichman, G. Grinstein, and D. S. Fisher, Phys. Rev. B **40**, 546 (1989).

[3] A. V. Chubukov, S. Sachdev, and J. Ye, Phys. Rev. B **49**, 11919 (1994).

[4] S. Sachdev, Phys. Rev. B **59**, 14054 (1999).

[5] W. Zwerger, Phys. Rev. Lett. **92**, 027203 (2004).

[6] T. Senthil, A. Vishwanath, L. Balents, S. Sachdev, and M. P. A. Fisher, Science **303**, 1490 (2004).

[7] D. Podolsky, A. Auerbach, and D. P. Arovas, Phys. Rev. B **84**, 174522 (2011).

[8] R. Coldea, D. A. Tennant, E. M. Wheeler, E. Wawrzynska, D. Prabhakaran, M. Telling, K. Habicht, P. Smeibidl, and K. Kiefer, Science **327**, 177 (2010).

[9] S. Sachdev, K. Sengupta, and S. M. Girvin, Phys. Rev. B **66**, 075128 (2002).

[10] J. Simon, W. S. Bakr, R. Ma, M. E. Tai, P. M. Preiss, and M. Greiner, Nature **472**, 307 (2011).

[11] Ch. Ruegg, B. Normand, M. Matsumoto, A. Furrer, D. F. McMorrow, K. W. Krämer, H.-U. Güdel, S. N. Gvasaliya, H. Mutka, and M. Boehm, Phys. Rev. Lett. **100**, 205701 (2008).

[12] D. S. Chow, P. Wzietek, D. Fogliatti, B. Alavi, D. J. Tantillo, C. A. Merlic, and S. E. Brown, Phys. Rev. Lett. **81**, 3984 (1998).

[13] M. Greiner, O. Mandel, T. Esslinger, T. W. Hänsch, and I. Bloch, Nature **415**, 39 (2002).

[14] I. B. Spielman, W. D. Phillips, and J. V. Porto, Phys. Rev. Lett. **98**, 080404 (2007).

[15] N. Gemelke, X. Zhang, C.-L. Hung, and C. Chin, Nature **460**, 995 (2009).

[16] J. F. Sherson, C. Weitenberg, M. Endres, M. Cheneau, I. Bloch I, S. Kuhr, Nature **467**, 68 (2010).

[17] W. S. Bakr, A. Peng, M. E. Tai, R. Ma, J. Simon, J. I. Gillen, S. Fölling, L. Pollet, M. Greiner, Science **329**, 547 (2010).

[18] M. Endres, M. Cheneau, T. Fukuhara, C. Weitenberg, P. Schauß, C. Gross, L. Mazza, M. C. Bañuls, L. Pollet, I. Bloch, S. Kuhr, Science **334**, 200 (2011).

[19] M. Endres, T. Fukuhara, D. Pekker, M. Cheneau, P. Schauß, C. Gross, E. Demler, S. Kuhr, and I. Bloch, Nature **487**, 454 (2012).

[20] K. G. Wilson and M. E. Fisher, Phys. Rev. Lett. **28**, 240 (1972).

[21] J. Oitmaa, Y. Kulik, and O. P. Sushkov, Phys. Rev. B **85**, 144431 (2012).

[22] S. Sachdev, *Quantum Phase Transitions*, Second Edition, Cambridge University Press, Cambridge UK (2011).

[23] N. H. Lindner and A. Auerbach, Phys. Rev. B **81**, 054512 (2010).

[24] E. Brezin, J. C. Le Guillou, and J. Zinn-Justin, in *Phase Transitions and Critical Phenomena*, edited by C. Domb and M. S. Green (Academic, New York), Vol. 6.

[25] L. Pollet and N. V. Prokof'ev, Phys. Rev. Lett. **109**, 010401 (2012).

[26] S. Sachdev, in *Quantum Theory of Condensed Matter*, Proceedings of the 24th Solvay Conference on Physics, Bertrand Halperin editor, World Scientific (2010), arXiv:0901.4103.

[27] T. Faulkner, Hong Liu, J. McGreevy, and D. Vegh, Phys. Rev. D **83**, 125002 (2011).

[28] F. Denef, S. A. Hartnoll, and S. Sachdev, Phys. Rev. D **80**, 126016 (2009).

[29] S. A. Hartnoll and D. M. Hofman, Phys. Rev. B **81**, 155125 (2010).

[30] R. Abe, Prog. Theor. Phys. **49**, 1877 (1973).

[31] Y. Okabe and M. Oku, Prog. Theor. Phys. **60**, 1277 (1978).